Received: 20 October 2022 | Revised: 25 January 2023 | Accepted: 28 January 2023

DOI: 10.1002/hyp.14820

RESEARCH ARTICLE

WILEY

On the variation of the correction factor of surface velocity with the measurement vertical for shallow flows over rough beds

Francesco Giuseppe Carollo[1] | Alessio Nicosia[1] | Vincenzo Palmeri[1] | Vincenzo Pampalone[1] | Vito Ferro[1,2]

[1]Department of Agricultural, Food and Forest Sciences, University of Palermo, Palermo, Italy

[2]NBFC, National Biodiversity Future Center, Palermo, Italy

Correspondence
Vincenzo Pampalone, Department of Agricultural, Food and Forest Sciences, University of Palermo, Viale Delle Scienze, Building 4, Palermo 90128, Italy.
Email: vincenzo.pampalone@unipa.it

Abstract

Considering that water flow energy affects the detachment of soil particles, the transport and deposit of the detached particles, the flow velocity is a key variable governing the soil erosion processes at the hillslope scale. The simple dye-tracer technique for measuring mean flow velocity can be applied in non-controlled field applications for which some measurement difficulties (e.g. due to sediment transport, and shallow flows) can occur. The correction factor is usually obtained as the ratio between the mean velocity, deriving from measurements of flow discharge and water depth, and surface velocity. Alternatively, the possibility of using the velocity profile in a given vertical to determine a suitable correction factor has not yet been explored. In this article, the flow velocity measurements were carried out in five verticals having a different distance from the wall of a flume whose bed was covered by hemispheres with different concentrations (9%–64%) and organized in two arrangements (square, staggered). Fifteen runs, characterized by different Reynolds and Froude numbers, were performed and the correction factor α_{vv} was calculated for each vertical. For the axial vertical α_{vv} was independent of the arrangement, decreased with the hemisphere concentration, and increased with both the Froude and Reynolds numbers. Furthermore, α_{vv} decreased from the bank to the flume axis as a result of the varying shape of the velocity profile. The analysis showed that the frequency distributions of the ratio between α_{vv} and its mean value α_m were overlaid and α_m was used to represent the correction factor, accordingly. A relation of α_m with the distance from the flume wall was detected. For the measured velocity profiles having a power shape, the analysis also demonstrated that the α_{vv} values, obtained by fitting the power law to the measurements, were close to both those calculated as the ratio between the mean velocity along the vertical and the surface velocity and their averaged values across the hydraulic section. These three methods give comparable average values of the correction factor, in the range of

0.72–0.75, which are close to the commonly applied value of 0.8. Finally, this investigation demonstrated that a single survey of a power velocity profile allows for obtaining the correction factor accounting for different verticals across the entire hydraulic section.

KEYWORDS

correction factor, dye method, flow velocity, measurement vertical, open channel flow, soil erosion, surface velocity, velocity distribution

1 | INTRODUCTION

Flow velocity is a key hydraulic variable affecting channelized (rills and gullies) and interrill erosion processes, and its knowledge and measurement are useful in developing and verifying process-based soil erosion models (Takken et al., 1998).

Although many measurement techniques are used to measure flow velocity in open channel flows (hot anemometry, particle imaging velocimetry-PIV, acoustic doppler velocimetry-ADV, infrared thermography, optical tacheometer) (Ali et al., 2012; Ayala et al., 2000; de Lima & Abrantes, 2014; Dunkerley, 2003; Giménez et al., 2004; Raffel et al., 1998), the dye-tracer technique is currently applied in overland (Dunkerley, 2001; Novak et al., 2017; Polyakov et al., 2021) and rill flows (Abrahams et al., 1996; Bagarello et al., 2015; Bruno et al., 2008; Di Stefano et al., 2015, 2017; Foster et al., 1984; Gilley et al., 1990; Govers, 1992; Line & Meyer, 1988). The main advantage of this technique is its simplicity (Wirtz et al., 2010, 2012) while more sophisticated methods (hot film anemometry, ADV and PIV) are suitable for controlled laboratory conditions (Ali et al., 2012) but their practical application in non-controlled field conditions can be difficult due to, for example, sediment transport and shallow flows (Liu et al., 2001; Planchon et al., 2005).

The dye-tracer technique is based on the injection of a tracer (Methylene blue, potassium permanganate, magnetic material, water isotope) (Berman et al., 2009; Dunkerley, 2003; Nicosia et al., 2021; Planchon et al., 2005; Ventura Jr. et al., 2001) in the flow, and the measurement of the travel time needed for the tracer to move from the injection section to a fixed downstream section (Chen et al., 2017). The ratio between the reach length and this travel time is equal to the surface flow velocity V_s.

The mean flow velocity V is obtained by correcting the measured V_s by a correction factor α_v (Zhang et al., 2010):

$$\alpha_v = \frac{V}{V_s}. \quad (1)$$

The main issue related to the dye-tracer technique is the choice of an appropriate value of α_v in different hydraulic conditions. Many theoretical and experimental investigations, with sediment-free and sediment-laden flows, have been developed for determining α_v.

For an infinitely wide laminar flow on a smooth and rigid bed, Horton et al. (1934) theoretically established $\alpha_v = 0.67$. Emmett (1970) carried out flume experiments and established that the correction factor increases with flow Reynolds number $Re = Vh/\nu_k$, in which h is the water depth, and ν_k is the kinematic viscosity, for transitional flows, while, α_v can be considered constant and equal to 0.8 for turbulent flow. For a sediment-free flow, Zhang et al. (2010) obtained an empirical relationship between the correction factor, slope and flow Reynolds number. Pan et al. (2015) experimentally investigated different roughness conditions and found that the correction factor is almost equal to 0.8 for turbulent flows. For sediment-free overland flows, Li and Abrahams (1997) found that α_v is not affected by slope, increases rapidly with Re in the transitional regime, while increases slowly with Re for turbulent flows.

Di Stefano et al. (2021) used a small flume with a fixed smooth bed simulating a rill channel, with slope s values from 0.1% to 8.7% and clear discharge Q ranging from 0.3 to 0.87 L s^{-1}, to compare a chronometer-based and a video-based technique for measuring the dye-tracer travel time. For the investigated condition, these authors obtained that α_v is independent of flow Reynolds number while is positively and linearly correlated with channel slope or a modified Froude number $F_s = V_s/(g\ h)^{0.5}$, in which g is the acceleration due to gravity and V_s replaces V.

Nicosia et al. (2021) carried out experiments using a sloping flume (5 m long, 0.078 m wide and 0.04 m high) simulating a rill channel with a rough bed and a sediment-free and turbulent flow to investigate the effects of grain roughness on α_v. The rill beds were covered with sieved soil having a median diameter d_{50} of 0.014 mm and gravel with $d_{50} = 4.7$ mm. The results of this investigation confirmed that α_v is independent of Re, as established by Di Stefano et al. (2021) for the smooth bed condition, while no relationship was found with F_s and channel slope. Moreover, the values of the correction factor for the gravel arrangement were higher than those obtained for the soil arrangement.

Li et al. (2022) performed overland flow experiments testing the effects of six surface roughness values, five rainfall intensities, 10 grass cover densities and three grass-shrub communities on the correction factor. For smooth surfaces, they found a negative correlation between α_v and the slope gradient (ranging from 8.7% to 42.26%) and no significant influence of Re on α_v. Their results also showed a significant negative correlation between α_v and roughness. Moreover, for both a smooth and rough surface, the correction factor increased with the rainfall intensity. For grass cover density lower than 3.45%, α_v increased with the cover density, while for values higher than 3.45%, the trend was the opposite. Finally, these authors presented a predictive equation of the correction factor, which considers the influence of rainfall intensity and roughness.

Summarizing, a common result of the aforementioned investigations is that α_v can be considered almost independent of *Re* for sediment-free turbulent flows.

Li et al. (1996) carried out flume experiments with transitional and turbulent flows on a mobile sand bed with *s* ranging from 4.7% to 17.7%. They obtained α_v values increasing with *Re* and an inverse empirical relationship of α_v with *s* (Li & Abrahams, 1997).

The experimental runs carried out by Ali et al. (2012) in a mobile bed flume allowed for establishing α_v values increasing with the size of the transported particles. Using measurements (Di Stefano et al., 2017, 2018a, 2018b) of surface flow velocity in eroding rills incised on plots having a mean slope equal to 9%, 14% and 22%, Di Stefano et al. (2018b) found that α_v can be assumed constant (0.665 or 0.80).

The effects of rill morphology and hydraulic characteristics on the correction factor α_v were experimentally investigated by Yang et al. (2020) for rill-free and rill flows. This investigation was performed using slope gradients in the 8.7%–46.6% range and laminar flows with Reynolds numbers ranging from 172 to 1040. The α_v values varied from 0.295 to 0.729 for rill-free flows and from 0.330 to 0.990 for rill flows. The correction factor α_v was affected by slope gradient and flow Reynolds number in the former case and by the rill depth and Reynolds number in the latter case.

In contrast to the fixed bed case, the correction factor on mobile beds was generally affected by the Reynolds number.

The available literature for different experimental conditions (sediment-free, sediment-laden, laminar, turbulent flows) supports the idea that using an appropriate correction factor of the surface velocity is a significant task in the fields of hydrometry, soil erosion and sediment transport.

The forementioned investigations were carried out by comparing the surface velocity V_s measured by the dye-tracer technique with the mean flow velocity *V* resulting from flow discharge and water depth measurements. In other words, the measured α_v values derived from a volumetric approach which characterizes the flow with only the mean flow velocity in the cross-section, *V*. This approach does not consider that the velocity profile depends on the measurement vertical in the cross-section and is characterized by a mean flow velocity V_v obtained by its integration. If the variability of the velocity distribution with the measurement vertical is considered, a correction factor, named α_{vv} and equal to V_v/V_s, can be defined for each vertical.

In a previous study, Di Stefano et al. (2020) used the velocity profiles measured in the channel axis by Ferro and Baiamonte (1994) and Coleman (1986) to test a theoretical relationship of α_{vv} versus the exponent of a fitting power law. Specifically, using the power velocity profile (Ferro, 2017, 2018)

$$\frac{v}{u_*}=\Gamma\left(\frac{u_* y}{\upsilon_k}\right)^{\delta}, \tag{2}$$

in which *v* is the local velocity, *y* is the distance from the bed, u_* is the shear velocity, Γ and δ are two parameters to be estimated for each measured velocity distribution, Di Stefano et al. (2020) obtained the following theoretical relationship:

$$\alpha_{vv}=\frac{1}{1+\delta}. \tag{3}$$

Di Stefano et al. (2020) established that, for sediment-free flows (Ferro & Baiamonte, 1994), α_{vv} increases with roughness height and is affected by the bed roughness characteristics (boulder size and concentration) while for the sediment-laden flows (Coleman, 1986) α_{vv} is inversely related to the sediment load (Li & Abrahams, 1997; Zhang et al., 2010).

The effect of roughness on the velocity distribution of shallow flows in natural hillslopes depends on the size of roughness elements. The latter ranges from grain to larger scales (e.g. gravel, stones and boulders), which cause different flow velocity distributions and, likely, different correction factor values. Most available investigations refer to the grain roughness case while scarce information concerns the study of the correction factor for shallow flows on rougher surfaces (e.g. Di Stefano et al., 2020; Fan et al., 2023). Fan et al. (2023) investigated element concentrations, ranging from 10% to 30%, by using hemispheres in a hexagonal pattern with a staggered structure glued on a sand bed. Two hydraulic conditions of submerged and non-submerged hemispheres were tested.

In this investigation, flume experiments are carried out for sediment-free flows over a rough bed made of hemispheres with square and staggered arrangements. The specific aims are to (i) evaluate the effect of the elements' arrangement and concentration, and the hydraulic characteristics on α_{vv}, (ii) analyse the influence of the measurement vertical on the velocity distribution and the related α_{vv}, (iii) analyse the variability of the mean value of α_{vv} across the section and (iv) compare the methods applied to calculate the correction factor.

2 | MATERIALS AND METHODS

The experimental runs were carried out using a flume having a slope of 0.005 (Figure 1), 14.4 m long, 0.6 m wide and 0.6 m deep, located at the Hydraulics Laboratory of the University of Palermo (Carollo & Ferro, 2021). The flume had glass bed and walls. The measuring reach, 3 m long, was located at 7.9 m from the entrance section to avoid large-scale disturbances. This experimental reach was covered with PVC hemispheres with a diameter of 0.06 m, and a height k_s of 0.03 m. The hemispheres were glued to the flume bed in a square arrangement, characterized by the same transversal and longitudinal distance between two elements (Figure 2a) and a staggered one (Figure 2b). Water discharge was measured by a concentric orifice plate installed in the feed pipe. The water depth *h* was measured relatively to the glass bed by a point gauge. The hemisphere concentration C_h was defined as the ratio between the horizontal projection area of the hemispheres and that of the measuring reach. The

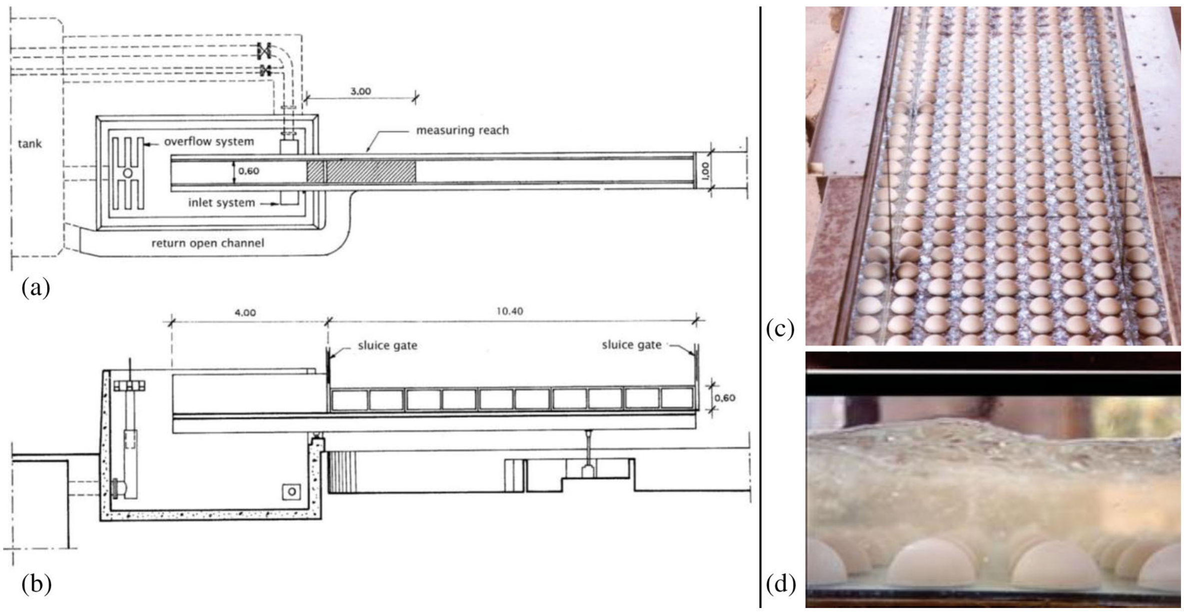

FIGURE 1 (a) Plan and (b) longitudinal view of the flume, and view of (c) an example of hemispheres' square arrangement and (d) flow during an experimental run.

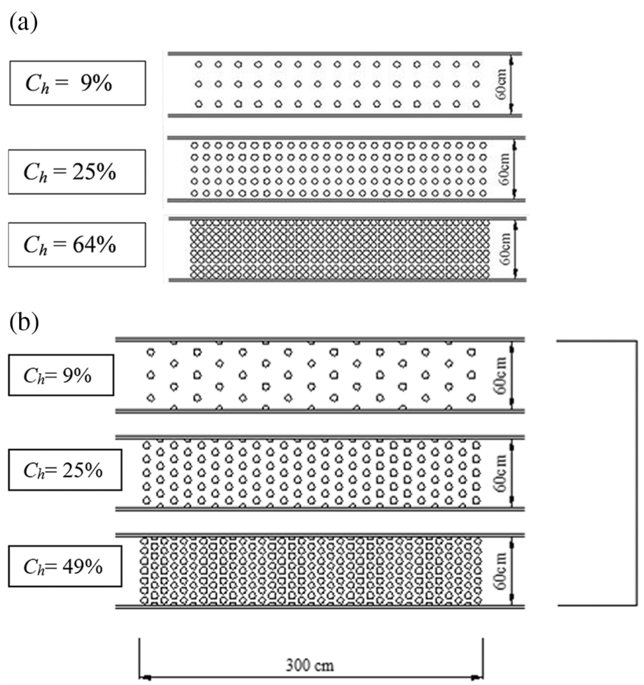

FIGURE 2 Scheme of the investigated hemisphere concentrations for (a) square and (b) staggered arrangements.

TABLE 1 Characteristic data of the experimental runs

Run	Arrangement	h/k_s	C_h (%)	*Re*	*F*
R1	Square	1.68	64	13 116	0.47
R2	Square	2.61	64	36 785	0.68
R3	Square	3.06	25	45 272	0.66
R4	Square	1.58	25	8238	0.32
R5	Square	5.17	25	115 692	0.77
R6	Square	3.20	9	59 016	0.81
R7	Square	1.67	9	14 646	0.53
R8	Staggered	5.94	9	159 957	0.87
R9	Staggered	3.16	9	57 656	0.80
R10	Staggered	1.57	9	11 207	0.45
R11	Staggered	6.13	25	119 000	0.61
R12	Staggered	2.99	25	40 015	0.61
R13	Staggered	6.00	49	133 437	0.71
R14	Staggered	3.17	49	38 237	0.53
R15	Staggered	1.71	49	8814	0.31

sediment/depth ratio h/k_s varied from 1.57 to 6.13 (Table 1), which are expressive values of shallow flows over submerged rough beds.

For each run, the velocity profiles were measured in five verticals of a cross-section located in the middle of the measuring reach. The measurement verticals were located at a distance *x* from the flume wall of 4 cm (V1 site), 8 cm (V2), 14 cm (V3), 21.5 cm (V4) and 30 cm (axial vertical, Va) (Figure 3) to explore the entire half-cross-section. Considering the expected symmetry of the flow, the investigated half-cross section is also representative of the other half. The local flow velocities were measured by a 2D side-looking probe ADV manufactured by SonTek Inc. (Kraus et al., 1994). It was mounted on a coordinate meter allowing the probe to move from one measurement vertical to another and, in a given vertical, to go down and up from one measurement point to another. The measurement accuracy is 0.1 mm/s for velocity values lower than 2.5 m/s and the error is always less than ±0.25%. Details on the instrument and the applied technique are reported in Ferro (2003).

Seven runs with different C_h (9%, 25% and 64%) were performed for the square arrangement, and eight runs, with C_h = 9%, 25% and 49%, were performed for the staggered one. The C_h values cover a

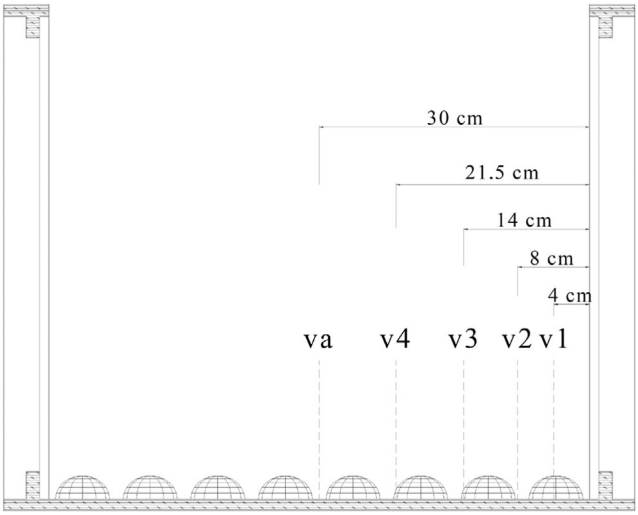

FIGURE 3 Locations of the investigated measurement verticals.

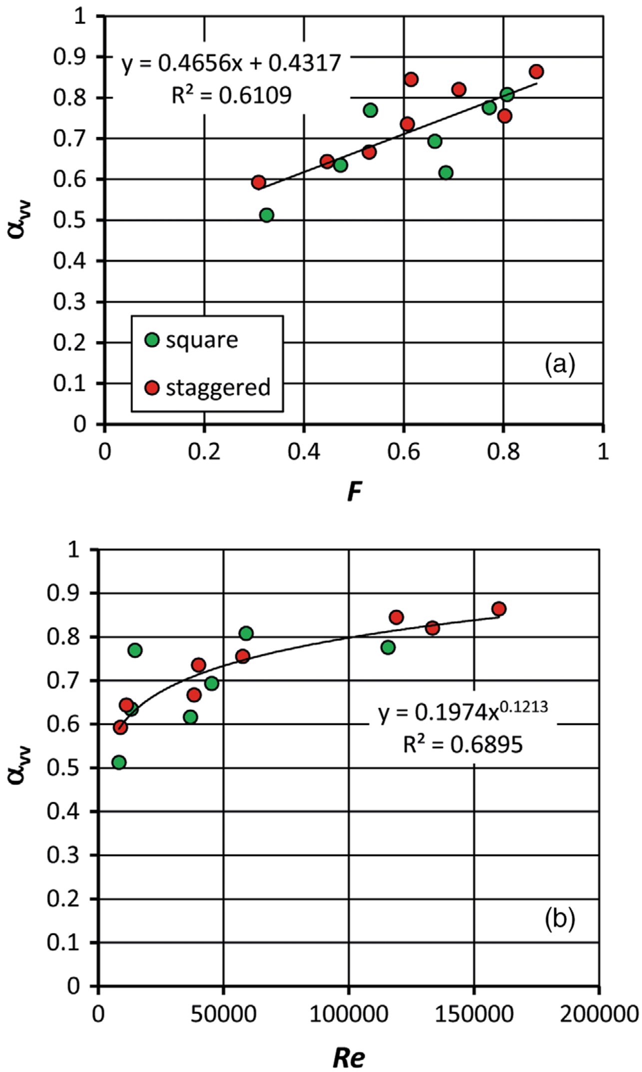

FIGURE 4 Relationship between the correction factor α_{vv} calculated for the axial vertical and (a) the Froude number and (b) the Reynolds number.

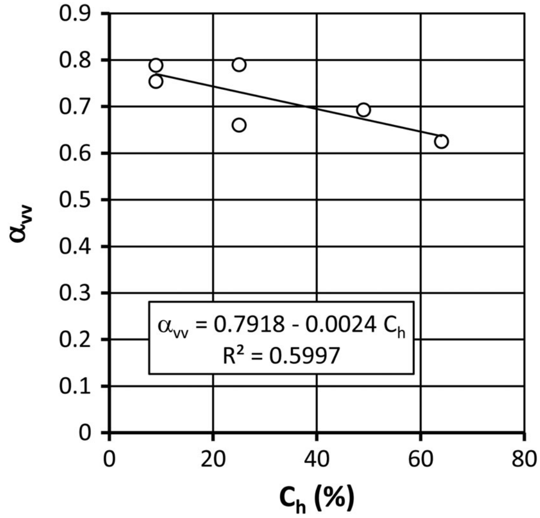

FIGURE 5 Relationship between the correction factor α_{vv} calculated for the axial vertical and the concentration C_h of hemispheres.

wide range of natural concentrations. Two different arrangements were set as this qualitative variable, together with roughness height and concentration, allows for fully characterizing roughness geometry.

For each run, Table 1 lists the investigated arrangement, the sediment/depth ratio h/k_s, the concentration C_h, the flow Reynolds number Re and the Froude number $F = V/(g\ h)^{0.5}$. The experimental runs were carried out for turbulent ($8238 \le Re \le 159\ 957$) and subcritical ($0.31 \le F \le 0.87$) flows.

3 | RESULTS

3.1 | Effect of element arrangement and concentration, and flow characteristics on α_{vv} related to the axial vertical

Figure 4 shows the variability of the correction factor α_{vv} with the Froude number (Figure 4a) and the Reynolds number (Figure 4b). This figure demonstrates that no appreciable difference exists between the two investigated arrangements (square, staggered) in the range of measured α_{vv} (0.51–0.81 for the square arrangement and 0.59–0.86 for the staggered one). Moreover, α_{vv} increases linearly with F and according to a power relationship of Re.

Figure 5 shows that a relationship exists between the correction factor α_{vv}, calculated by averaging the α_{vv} values corresponding to a given arrangement and concentration, and C_h.

3.2 | Assessing the influence of the measurement vertical on the correction factor

For studying the influence of the measurement vertical on the velocity distribution and the related correction factor, the frequency

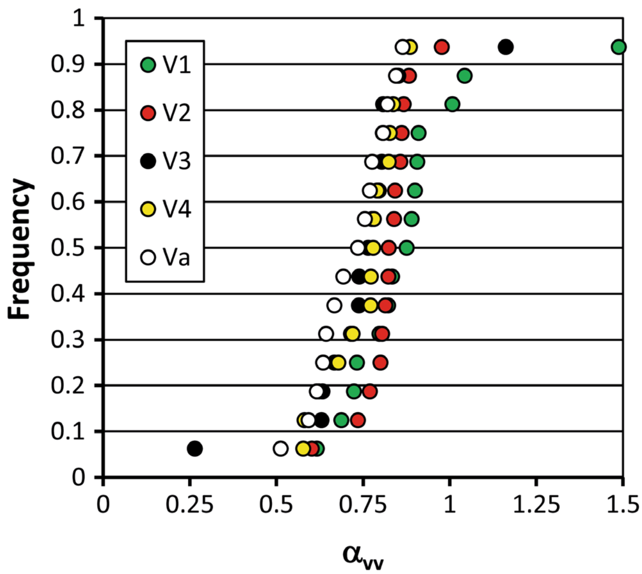

FIGURE 6 Frequency distributions of the correction factor α_{vv} determined in the different measurement verticals.

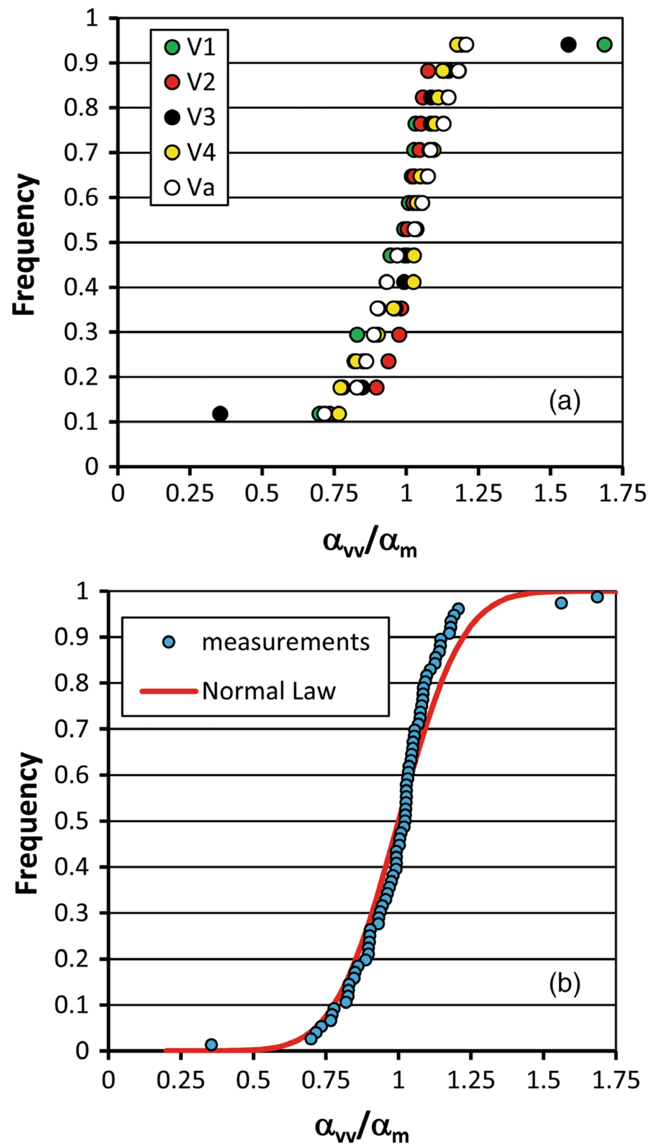

FIGURE 7 Frequency distributions of the α_{vv}/α_m ratio for (a) each investigated vertical and (b) all the measurements put together.

TABLE 2 Characteristic data of the frequency distribution of α_{vv} for each measurement vertical

Vertical	V1	V2	V3	V4	Va
Minimum	0.62	0.60	0.26	0.58	0.51
Maximum	1.49	0.98	1.16	0.89	0.86
Mean α_m	0.88	0.82	0.74	0.75	0.72
Median	0.88	0.82	0.76	0.78	0.74
Standard deviation	0.20	0.08	0.18	0.10	0.10

distributions of α_{vv} measured in the 15 runs were plotted in Figure 6. The main statistics of each frequency distribution are listed in Table 2.

Figure 6 clearly demonstrates that the frequency distribution of α_{vv} depends on the measurement vertical and the correction factor values decrease from the channel bank (V1) to the axis (Va). The frequency distribution of the α_{vv}/α_m ratio, in which α_m is the average of the 15 α_{vv} values, was also investigated. Figure 7a demonstrates that the five frequency distributions are overlaid and can be considered independent of the measurement vertical. In other words, these empirical distributions are sampled from the same population. Putting together all the available data (75 measurements, Figure 7b) α_{vv}/α_m is distributed according to the normal law with sample mean and standard deviation equal to 1 and 0.174, respectively. According to this result, the correction factor α_{vv} can be represented by its mean value α_m. This mean value varies with the dimensionless distance $2x/B$ from the flume wall, in which B is the channel width, according to the following relationship (Figure 8):

$$\alpha_m = 0.713\left(\frac{2x}{B}\right)^{-0.102}. \tag{4}$$

The reduction of α_m with the distance from the wall can be explained by considering the shape of the velocity profile. Figure 9 shows, for example for the experimental run R8 (Table 1), that the shape of the velocity profile is related to the considered vertical. Specifically, the velocity profile has a dip (the maximum velocity is sharply located below the water surface) in V1, while it often tends to a power shape, with the maximum velocity located at the water surface ($y = h$), in the other verticals.

3.3 | Testing different methods to calculate the correction factor

For 21 out of 45 profiles measured in Va, V4 and V3, the velocity distribution had a power shape and the correction factor α_{vv} was

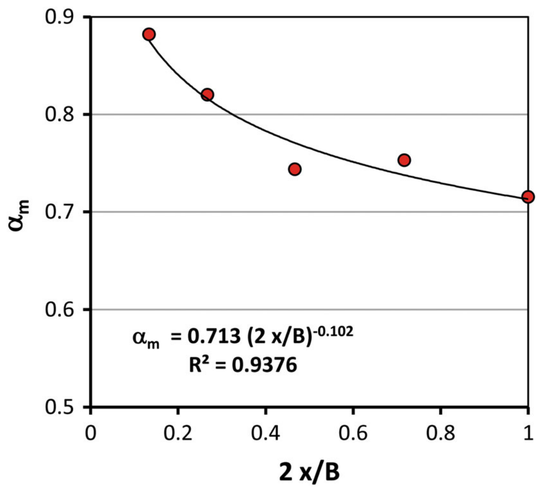

FIGURE 8 Relationship between the mean, α_m, of the 15 measured values of the correction factor in the measurement vertical and the dimensionless distance $2x/B$.

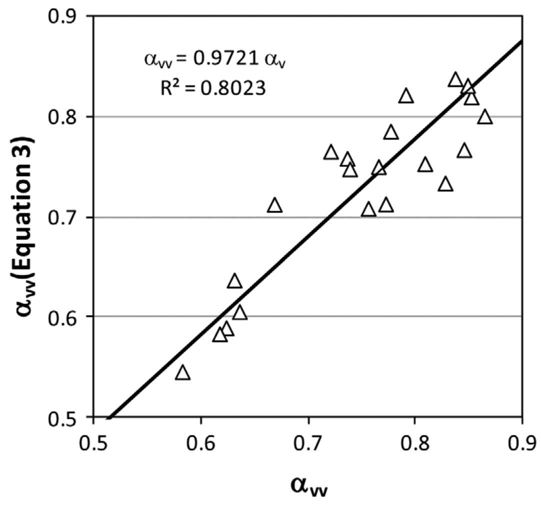

FIGURE 10 Comparison between the correction factor values $\alpha_v = V_v/V_s$ and those calculated by Equation (3).

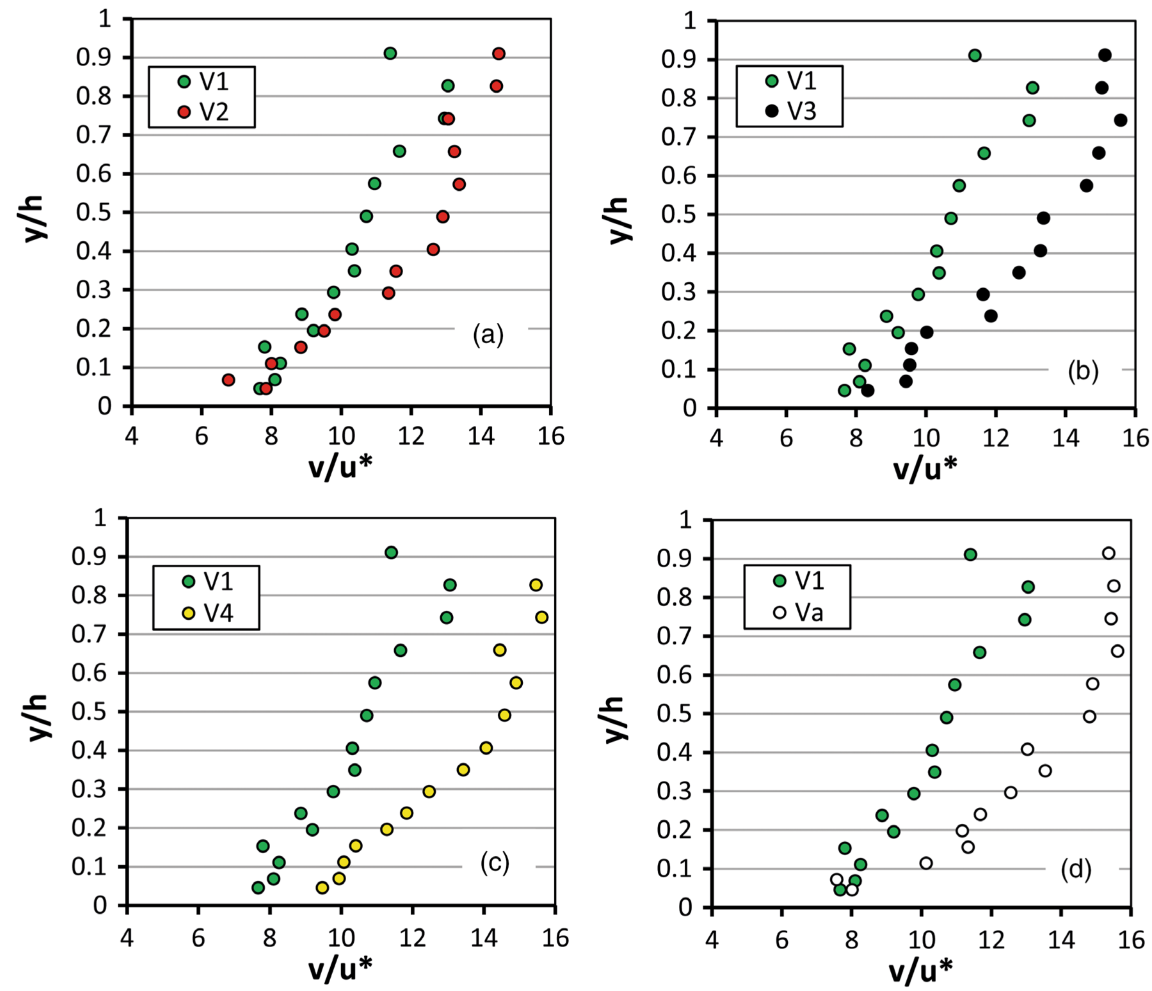

FIGURE 9 Comparison, for the run R8, between the velocity profile measured in the vertical V1 and those measured in the (a) V2, (b) V3, (c) V4 and (d) Va.

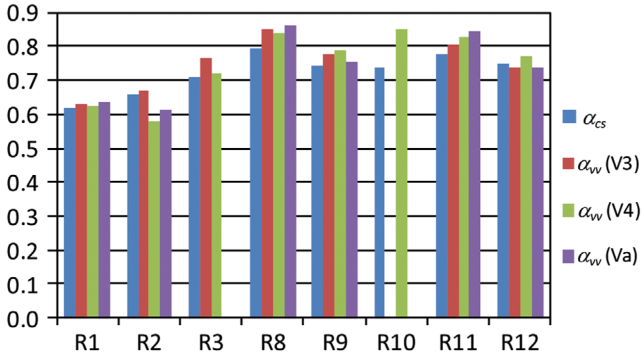

FIGURE 11 Comparison among $\alpha_{vv} = V_v/V_s$ related to V3, V4 and Va with power profiles and the corresponding α_{cs}.

TABLE 3 Characteristic data of the different correction factors related to the Va, V4 and V3 measurement verticals with a power velocity profile (α_{vv}) and the 15 runs (α_{cs})

Correction factor	$\alpha_{vv} = V_v/V_s$	α_{vv} (Equation 3)	α_{cs}
Minimum	0.58	0.55	0.57
Maximum	0.86	0.84	0.91
Mean	0.75	0.73	0.72
Median	0.76	0.75	0.74
Standard deviation	0.089	0.087	0.078

calculated by Equation (3). The comparison between the correction factor $\alpha_{vv} = V_v/V_s$ and α_{vv} calculated by Equation (3), is plotted in Figure 10. This Figure demonstrates that, when the measured velocity profile has a power shape, the correction factor calculated by Equation (3) is, on average, slightly less (97.2%) than that obtained by measured surface and mean flow velocities. This slight difference reflects the goodness of fit of the power distribution to the measured velocity profile. For each of the 15 experimental runs, a correction factor, named α_{cs}, was obtained by averaging the α_{vv} values across the hydraulic section under the hypothesis of a linear variation between verticals. For a given run, that is for fixed values of Froude and Reynolds numbers, Figure 11 shows the comparison among $\alpha_{vv} = V_v/V_s$ related to V3, V4 and Va with power profiles (21 velocity profiles) and the corresponding α_{cs}. The variations relative to α_{cs} are -11.7 (R2, V4) to 15.3% (R10, V4). The statistical parameters resulting from the 21 values of $\alpha_{vv} = V_v/V_s$, α_{vv} calculated by Equation (3), and the 15 values of α_{cs}, listed in Table 3, feature slight differences.

4 | DISCUSSION

4.1 | Effect of element arrangement and concentration, and flow characteristics on α_{vv} related to the axial vertical

The circumstance that the relationships between α_{vv} and the Froude number (Figure 4a) and the Reynolds number (Figure 4b) are independent of the hemisphere arrangement can be justified considering that, for low concentration values (9%–25%), the velocity distributions are similar while, for the highest values (49%–64%), the occurrence of the quasi-skimming flow regime limits the influence of the element arrangement (Carollo & Ferro, 2021; Morris, 1959). A slight effect of the Reynolds number on the correction factor was found by Fan et al. (2023) for transitional and turbulent shallow flows over a bed roughness due to hemisphere arrangement. This was the overall result obtained for two hydraulic conditions of submerged and non-submerged hemispheres. The present increasing relationship of α_{vv} versus *Re* contrasts with the finding by Fan et al. (2023) and with the result, generally obtained in the literature, that α_v is independent or weakly increasing with *Re* for turbulent sediment-free flows. However, all these literature results were obtained for different experimental conditions relative to those explored here (e.g. they are not based on measurements of velocity profiles or are also obtained from non-submerged flow conditions).

The result that the correction factor increased linearly with *F* aligns with the findings of Di Stefano et al. (2021), although they considered a modified Froude number, F_s, instead of *F*.

Figure 5 shows that α_{vv} decreases for increasing values of the hemisphere concentration C_h, similarly to what was highlighted by Di Stefano et al. (2020), and Fan et al. (2023) for transitional and turbulent flows.

4.2 | Assessing the influence of the measurement vertical on the correction factor

According to Figure 6, α_{vv} clearly depends on the measurement vertical, and declines from the channel bank (V1) to the axis (Va). This reduction can be explained by the shape of the velocity distribution (Figure 9), which has a dip and is more uniform close to the flume wall compared with the other measurement verticals. The variability of the α_{vv} values with the measurement vertical also determines the decreasing relationship of α_m against the distance from the flume wall (Figure 8).

For Va, V4 and V3, the mean values α_m listed in Table 2 (0.72, 0.75 and 0.74, respectively) are very close to the value of 0.752 determined by Di Stefano et al. (2020) for sediment-free flows over a rough bed. The three ranges of the correction factor (Table 2) are partially overlapped with that (0.46–0.78) obtained by Fan et al. (2023) for transitional and turbulent flows, and α_m is always higher than the mean value of 0.61 related to this literature study. However, as outlined above, this comparison is not rigorous in terms of both hydraulic conditions and channel slope. Indeed, the present sediment/depth ratio h/k_s varies from 1.57 to 6.13 (submerged flow), while the complete dataset by Fan et al. (2023) features h/k_s ranging approximately from 0.3 to 1.7 (non-submerged and submerged flows). The channel slope is also very different, as it is equal to 0.5% here, while it ranges from 7% to 17.6% for the literature dataset.

4.3 | Testing different methods to calculate the correction factor

For the power velocity profiles measured in Va, V4 and V3, the analysis demonstrated that Equation (3) gives α_{vv} values slightly different from those $\alpha_{vv} = V_v/V_s$. This result is due to the circumstance that the velocity profiles were well described by the theoretical power velocity distribution and the more this power distribution fits the measured velocity profile, the more α_{vv} (calculated by Equation (3)) gets close to $\alpha_{vv} = V_v/V_s$. The plot of Figure 11 and the detected percentage differences between α_{vv} and α_{cs} support the conclusion that α_{vv} varies between runs and a single survey of a power velocity profile relatively close to the axial vertical is enough to obtain the correction factor accounting for different verticals across the entire section. By neglecting the dependence of α_{vv} on the experimental run, an average correction factor in the range of 0.72–0.75 (with a standard deviation of 0.078–0.089) (Table 3), which is close to the usual value of 0.8, can be assumed for applying the three tested methods for turbulent shallow flows over rough beds.

5 | CONCLUSIONS

Even though the dye-tracer technique is currently applied, its reliability is affected by the choice of appropriate α_v values for different hydraulic conditions to correct the measured surface velocity V_s.

For the investigated concentrations, the analysis demonstrated that the correction factor α_{vv} calculated for the axial velocity profile is independent of the arrangement, decreases with C_h and increases for increasing values of the Froude and Reynolds numbers. As a consequence of the velocity profile shape, α_{vv} decreases from the channel bank to the axis resulting in a decreasing relationship of α_m against the distance from the flume wall. This mean value is representative of the correction factor as the frequency distributions of the ratio α_{vv}/α_m corresponding to the investigated verticals are overlaid and normally distributed.

For the measured power velocity profiles, the analysis also confirmed the applicability of the theoretical expression (Equation 3) of the correction factor and suggested that a single survey of a power velocity profile, which is likely to occur close to the axial vertical, is enough to determine the correction factor.

Finally, under the hypothesis of neglecting the dependence of α_{vv} on the experimental run, the applied methods to calculate the correction factor gave comparable average values, in the range of 0.72–0.75, which are close to the commonly applied value of 0.8.

ACKNOWLEDGEMENTS

All the Authors developed the theoretical analysis, analysed the results and contributed to writing the article. This research did not receive any specific grant from funding agencies in the public, commercial, or not-for-profit sectors. Open Access Funding provided by Universita degli Studi di Palermo within the CRUI-CARE Agreement.

DATA AVAILABILITY STATEMENT

The data that support the findings of this study are available from the corresponding author upon reasonable request.

ORCID

Francesco Giuseppe Carollo https://orcid.org/0000-0001-9782-998X
Alessio Nicosia https://orcid.org/0000-0003-0540-8788
Vincenzo Palmeri https://orcid.org/0000-0001-6594-9530
Vincenzo Pampalone https://orcid.org/0000-0002-5195-9209
Vito Ferro https://orcid.org/0000-0003-3020-3119

REFERENCES

Abrahams, A. D., Li, G., & Parsons, A. J. (1996). Rill hydraulics on a semiarid hillslope, southern Arizona. *Earth Surface Processes and Landforms*, *21*, 35–47.

Ali, M., Sterk, G., Seeger, M., & Stroosnijder, L. (2012). Effect of flow discharge and median grain size on mean flow velocity under overland flow. *Journal of Hydrology*, *452-453*, 150–160.

Ayala, J. E., Martinez-Austria, P., Menendez, J. R., & Segura, F. A. (2000). Fixed bed forms laboratory channel flow analysis. *Ingenieria Hidraulica En Mexico*, *15*(2), 75–84.

Bagarello, V., Di Stefano, C., Ferro, V., & Pampalone, V. (2015). Establishing a soil loss threshold for limiting rilling. *Journal of Hydrologic Engineering, ASCE*, *20*(C6014001), 1–5.

Berman, E. S. F., Gupta, M., Gabrielli, C., Garland, T., & McDonnell, J. J. (2009). High-frequency field deployable isotope analyzer for hydrological applications. *Water Resources Research*, *45*(W10201), 1–7.

Bruno, C., Di Stefano, C., & Ferro, V. (2008). Field investigation on rilling in the experimental Sparacia area, South Italy. *Earth Surface Processes and Landforms*, *33*, 263–279.

Carollo, F. G., & Ferro, V. (2021). Experimental study of boulder concentration effect on flow resistance in gravel bed channels. *Catena*, *205*, 105458.

Chen, C., Ban, Y., Wang, X., & Lei, T. (2017). Measuring flow velocity on frozen and non-frozen slopes of black soil through leading edge method. *International Soil and Water Conservation Research*, *5*, 180–189.

Coleman, N. L. (1986). Effects of suspended sediment on the open-channel velocity distribution. *Water Resources Research*, *22*, 1377–1384.

de Lima, J. L. M. P., & Abrantes, J. R. C. B. (2014). Using a thermal tracer to estimate overland and rill flow velocities. *Earth Surface Processes and Landforms*, *39*, 1293–1300.

Di Stefano, C., Ferro, V., Palmeri, V., & Pampalone, V. (2017). Flow resistance equation for rills. *Hydrological Processes*, *31*, 2793–2801.

Di Stefano, C., Ferro, V., Palmeri, V., & Pampalone, V. (2018a). Testing slope effect on flow resistance equation for mobile bed rills. *Hydrological Processes*, *32*, 664–671.

Di Stefano, C., Ferro, V., Palmeri, V., & Pampalone, V. (2018b). Assessing dye-tracer technique for rill flow velocity measurements. *Catena*, *171*, 523–532.

Di Stefano, C., Ferro, V., & Pampalone, V. (2015). Modeling rill erosion at the Sparacia experimental area. *Journal of Hydrologic Engineering, ASCE*, *20*(C5014001), 1–12.

Di Stefano, C., Nicosia, A., Palmeri, V., Pampalone, V., & Ferro, V. (2020). Dye-tracer technique for rill flows by velocity profile measurements. *Catena*, *185*(104313), 1–7.

Di Stefano, C., Nicosia, A., Palmeri, V., Pampalone, V., & Ferro, V. (2021). Flume experiments for assessing the dye-tracing technique in rill flows. *Flow Measurement and Instrumentation*, *77*(2), 101870.

Dunkerley, D. L. (2001). Estimating the mean speed of laminar overland flow using dye injection-uncertainty on rough surfaces. *Earth Surface Processes and Landforms*, *26*, 363–374.

Dunkerley, D. L. (2003). An optical tachometer for short-path measurement of flow speeds in shallow overland flows: Improved alternative to dye timing. *Earth Surface Processes and Landforms*, *28*, 777–786.

Emmett, W. W. (1970). The hydraulics of overland flow on hillslopes. U.S. Geological Survey Professional Papers 622-A.

Fan, D., Yu, X., Jia, G., Zheng, P., & Wu, N. (2023). Correction factor for determining mean velocity of shallow flow on rough surfaces under varying inundation conditions using dye tracer method, accepted for publication on Earth surface Processes and Landforms. https://doi.org/10.1002/esp.5544

Ferro, V. (2003). Flow resistance in gravel-bed channels with large-scale roughness. *Earth Surface Processes and Landforms*, *28*(12), 1325–1339.

Ferro, V. (2017). New flow resistance law for steep mountain streams based on velocity profile. *Journal of Irrigation and Drainage Engineering*, *143*, 1–6.

Ferro, V. (2018). Assessing flow resistance in gravel bed channels by dimensional analysis and self-similarity. *Catena*, *169*, 119–127.

Ferro, V., & Baiamonte, G. (1994). Flow velocity profiles in gravel-bed rivers. *Journal of Hydraulic Engineering, ASCE*, *120*(1), 60–80.

Foster, G. R., Huggins, L. F., & Meyer, L. D. (1984). A laboratory study of rill hydraulics: I. Velocity Relationships. *Transactions of the ASAE*, *27*, 790–796.

Gilley, J. E., Kottwitz, E. R., & Simanton, J. R. (1990). Hydraulics characteristics of rills. *Transaction of the ASAE*, *27*, 797–804.

Giménez, R., Planchon, O., Silvera, N., & Govers, G. (2004). Longitudinal velocity patterns and bed morphology intercation in a rill. *Earth Surface Processes and Landforms*, *29*, 105–114.

Govers, G. (1992). Relationship between discharge, velocity and flow area for rills eroding loose, non-layered materials. *Earth Surface Processes and Landforms*, *17*, 515–528.

Horton, R. E., Leach, H. R., & Vliet, V. R. (1934). Laminar sheet flow. *Transactions of the American Geophysical Union*, *15*, 393–404.

Kraus, N. C., Lohrmann, A., & Cabrera, R. (1994). New acoustic meter for measuring 3D laboratory flows. *ASCE Journal of Hydraulic Engineering*, *120*(3), 406–412.

Li, G., & Abrahams, A. D. (1997). Effect of salting sediment load on the determination of the mean velocity of overland flow. *Water Resources Research*, *33*, 341–347.

Li, G., Abrahams, A. D., & Atkinson, J. F. (1996). Correction factors in the determination of mean flow velocity of overland flow. *Earth Surface Processes and Landforms*, *21*, 509–515.

Li, P., Zhang, K., Xu, Q., Lv, X., Ling, P., Cen, Y., & Shang, H. (2022). Experimental study on the correction factor of surface overland flow velocity. *Catena*, *218*, 106576.

Line, D. E., & Meyer, L. D. (1988). Flow velocities of concentrated runoff along cropland furrows. *Transactions of the ASAE*, *31*, 1435–1439.

Liu, Z., Adrian, R. J., & Hanratty, T. J. (2001). Large-scale modes of turbulent channel flow: Transport and structure. *Journal of Fluid Mechanics*, *448*, 53–80.

Morris, H. M. (1959). Design methods for flow in rough conduits. *ASCE Journal of the Hydraulics Division*, *85*(7), 43–62.

Nicosia, A., Di Stefano, C., Palmeri, V., Pampalone, V., & Ferro, V. (2021). Roughness effect on the correction factor of surface velocity for rill flows. *Hydrological Processes*, *35*(10), e14407.

Novak, G., Rak, G., Prešeren, T., & Bajcar, T. (2017). Non-intrusive measurements of shallow water discharge. *Flow Measurement and Instrumentation*, *56*, 14–17.

Pan, C., Shangguan, Z., & Ma, L. (2015). Assessing the dye-tracer correction factor for documenting the mean velocity of sheet flow over smooth and grassed surfaces. *Hydrological Processes*, *29*, 5369–5382.

Planchon, O., Silvera, N., Giménez, R., Favis-Mortlock, D., Wainwright, J., Le Bissonnais, Y., & Govers, G. (2005). An automated salt-tracing gauge for flow-velocity measurement. *Earth Surface Processes and Landforms*, *30*, 833–844.

Polyakov, V., Li, L., & Nearing, M. A. (2021). Correction factor for measuring mean overland flow velocities on stony surfaces under rainfall using dye tracer. *Geoderma*, *390*, 114975.

Raffel, M., Willert, C., & Kompnhans, J. (1998). *Particle image velocimetry. In a practical guide (experimental fluid mechanics)*. Springer.

Takken, I., Govers, G., Ciesiolka, C. A. A., Silburn, D. M., & Loch, R. J. (1998). Factors influencing the velocity-discharge relationship in rills. In *Modelling soil erosion, sediment transport and closely related hydrological processes* (pp. 63–69). International Association of Hydrological Sciences Publ. N. 249.

Ventura, E., Jr., Nearing, M. A., & Norton, L. D. (2001). Developing a magnetic tracer to study soil erosion. *Catena*, *43*, 277–291.

Wirtz, S., Seeger, M., & Ries, J. B. (2010). The rill experiment as a method to approach a quantification of rill erosion process activity. *Zeitschrift für Geomorphologie*, *54*, 47–64.

Wirtz, S., Seeger, M., & Ries, J. B. (2012). Field experiment for understanding and quantification of rill erosion processes. *Catena*, *91*, 21–34.

Yang, D. M., Fang, N. F., & Shi, Z. H. (2020). Correction factor for rill flow velocity measured by the dye tracer method under varying rill morphologies and hydraulic characteristics. *Journal of Hydrology*, *591*, 125560.

Zhang, G., Luo, R., Cao, Y., Shen, R., & Zhang, X. C. (2010). Correction factor to dye-measured flow velocity under varying water and sediment discharges. *Journal of Hydrology*, *389*, 205–213.

How to cite this article: Carollo, F. G., Nicosia, A., Palmeri, V., Pampalone, V., & Ferro, V. (2023). On the variation of the correction factor of surface velocity with the measurement vertical for shallow flows over rough beds. *Hydrological Processes*, *37*(2), e14820. https://doi.org/10.1002/hyp.14820